Am J Physiol Heart Circ Physiol 284: H92–H100, 2003.
First published September 12, 2002; 10.1152/ajpheart.00330.2002.

VEGF increases endothelial permeability by separate signaling pathways involving ERK-1/2 and nitric oxide

JEROME W. BRESLIN, PETER J. PAPPAS, JOAQUIM J. CERVEIRA,
ROBERT W. HOBSON II, AND WALTER N. DURÁN
Program in Vascular Biology and Division of Vascular Surgery, Department of Pharmacology and Physiology and Department of Surgery, New Jersey Medical School, University of Medicine of New Jersey, Newark, New Jersey 07101-1709

Submitted 15 April 2002; accepted in final form 6 September 2002

Breslin, Jerome W., Peter J. Pappas, Joaquim J. Cerveira, Robert W. Hobson II, and Walter N. Durán. VEGF increases endothelial permeability by separate signaling pathways involving ERK-1/2 and nitric oxide. *Am J Physiol Heart Circ Physiol* 284: H92–H100, 2003. First published September 12, 2002; 10.1152/ajpheart.00330.2002.—We tested the hypothesis that VEGF regulates endothelial hyperpermeability to macromolecules by activating the ERK-1/2 MAPK pathway. We also tested whether PKC and nitric oxide (NO) mediate VEGF-induced increases in permeability via the ERK-1/2 pathway. FITC-Dextran 70 flux across human umbilical vein endothelial cell monolayers served as an index of permeability, whereas Western blots assessed the phosphorylation of ERK-1/2. VEGF-induced hyperpermeability was inhibited by antisense DNA oligonucleotides directed against ERK-1/2 and by blockade of MEK and Raf-1 activities (20 μM PD-98059 and 5 μM GW-5074). These blocking agents also reduced ERK-1/2 phosphorylation. The PKC inhibitor bisindolylmaleimide I (10 μM) blocked both VEGF-induced ERK-1/2 activation and hyperpermeability. The NO synthase (NOS) inhibitor N^G-nitro-L-arginine methyl ester (200 μM) and the NO scavenger 2-phenyl-4,4,5,5-tetramethylimidiazoline-1-oxyl-3-oxide (100 μM) abolished VEGF-induced hyperpermeability but did not block ERK-1/2 phosphorylation. These observations demonstrate VEGF-induced hyperpermeability involves activation of PKC and NOS as well as Raf-1, MEK, and ERK-1/2. Furthermore, our data suggest that ERK-1/2 and NOS are elements of different signaling pathways in VEGF-induced hyperpermeability.

microvascular permeability; mitogen-activated protein kinases; endothelial cells; vascular endothelial growth factor; protein kinase C

THE ENDOTHELIUM of capillaries and postcapillary venules forms a semipermeable barrier that coordinates exchange between the bloodstream and tissues in response to changing tissue environments. Inflammatory mediators compromise this barrier function, resulting in increased permeability and tissue edema. VEGF is the most potent stimulator of permeability currently known, being 50,000 times more potent than histamine (13, 36). VEGF is released by hypoxic or injured tissues and increases nutrient delivery by increasing blood flow and microvascular permeability and by promoting angiogenesis (4, 38).

VEGF binds to at least two transmembrane tyrosine kinase receptors on endothelial cells, named Flt-1 (VEGF receptor-1) and Flk-1/KDR (VEGF receptor-2) (27, 32). Binding of VEGF to KDR results in tyrosine phosphorylation and activation of phosphatidylinositol 3-kinase (PI3K) (17) and phospholipase C-γ (PLC-γ) (17, 23, 28, 45). PLC-γ causes the formation of diacylgylcerol and inositol (1,4,5)-trisphosphate, which activate PKC and the release of Ca^{2+} from internal stores, respectively (7). There is evidence, however, that VEGF mediates increases in Ca^{2+} by increasing Ca^{2+} flux across the plasma membrane (8). PI3K stimulation results in activation of Akt (14). PKC, calcium, and Akt all activate endothelial nitric oxide (NO) synthase (eNOS), leading to increased NO release, which is associated with vasodilation and increased vascular permeability (11, 15, 20, 26, 33). A role for PLC-γ, PKC, calcium, and NO in VEGF-induced hyperpermeability has been confirmed in isolated coronary venules (45), and the involvement of PI3K/Akt and NO was demonstrated in human umbilical vein endothelial cell (HUVEC) monolayers (25).

Studies with pharmacological inhibitors have suggested a role for the p42/44 MAPKs (also known as ERK-1/2) in VEGF-induced hyperpermeability (5, 21, 25). Growth factors are thought to activate ERK-1/2 through the Ras-Raf-MEK pathway (9). There is evidence, however, that VEGF-induced ERK-1/2 activation occurs via Ras-independent pathways involving PKC (12, 39) and PKG (30). We have previously shown that blockade of ERK-1/2 with AG-126 inhibits hyperpermeability in response to the PKG activator 8-bromo-cGMP (30). In addition, phorbol ester-mediated activation of ERK-1/2 and hyperpermeability involves PKC and Ras (43). No study to date, however, has examined the upstream mediators of ERK-1/2 in VEGF-mediated hyperpermeability.

Address for reprint requests and other correspondence: W. N. Durán, Dept. of Pharmacology and Physiology, UMDNJ, New Jersey Medical School, 185 South Orange Ave., MSB H-633, PO Box 1709, Newark, NJ 07101-1709 (E-mail: duran@umdnj.edu).

The costs of publication of this article were defrayed in part by the payment of page charges. The article must therefore be hereby marked "*advertisement*" in accordance with 18 U.S.C. Section 1734 solely to indicate this fact.

To advance knowledge on the role of ERK-1/2 in VEGF-induced hyperpermeability, we depleted ERK-1/2 from endothelial cells using an approach based on antisense oligonucleotides. We also tested the role of MEK and Raf-1, two upstream regulators of ERK-1/2 activity, in VEGF-induced hyperpermeability. In addition, we tested whether PKC and NOS significantly modulate VEGF-mediated ERK-1/2 phosphorylation. Our data demonstrate that VEGF increases permeability by at least two different pathways: one involving Raf-1, MEK, and ERK-1/2; and the other involving NOS. We also demonstrate that PKC, which increases permeability via increased NO production (20, 33), is a mediator of VEGF-induced ERK-1/2 phosphorylation and hyperpermeability.

MATERIALS AND METHODS

Reagents and antibodies. Endothelial growth medium (EGM) and serum-free endothelial basal medium (EBM) were obtained from Clonetics (San Diego, CA). Fibronectin, OptiMEM, and trypsin-EDTA were from Life Technologies (Grand Island, NY). PD-98059 was from BioMol (Plymouth Meeting, PA). Raf-1 kinase inhibitor I (GW-5074), bisindolylmaleimide (BIM) I, BIM V, *S*-nitroso-*N*-acetyl penicillamine (SNAP), and 2-phenyl-4,4,5,5-tetramethylimidazoline-1-oxyl-3-oxide (PTIO) were from Calbiochem (San Diego, CA). TransIT-LT-1 polyamine transfection reagent was from Mirus (Madison, WI). The enhanced chemiluminescence (ECL) detection kit was from Amersham (Buckinghamshire, UK). VEGF, antibodies to ERK-1/2, diphosphorylated (Thr-183 and Tyr-185) ERK-1/2, horseradish peroxidase-conjugated anti-rabbit IgG, anti-mouse IgG secondary antibodies, FITC-labeled Dextran 70 (FITC-Dx 70), N^G-nitro-L-arginine methyl ester (L-NAME), bicinchoninic acid protein assay reagents, and all other reagents, unless specified, were from Sigma.

Cell cultures. Primary HUVEC were obtained from Clonetics. HUVEC were grown in EGM at 37°C under 5% CO_2-95% air. Cells were passaged by trypsinization with trypsin-EDTA and were seeded onto fibronectin-coated, 12-mm-diameter, 0.4-μm pore Snapwell polycarbonate membranes (Costar; Cambridge, MA) for permeability experiments. Cells used for immunoblot analysis were grown in six-well tissue culture plates. All experiments used *passages 2–4* HUVEC.

Endothelial monolayer permeability experiments. The HUVEC monolayer permeability model has been previously described (25, 42). Briefly, HUVEC were grown on fibronectin-coated polycarbonate membranes for 6–7 days to achieve confluence. The membranes were rinsed with phenol red-free (PRF) EBM (EBM Clonetics) and inserted between two chambers of a prewarmed diffusion system (Navicyte; San Diego, CA). For operational purposes, the chamber facing the side on which the cells were grown is referred to as the "luminal" side and the other chamber as the "abluminal" side. The temperature of the system was maintained at 37°C by a circulating water bath, and the pH of the media was maintained at 7.4 by bubbling of 5% CO_2-95% N_2. The bubbling also served to stir the medium. The system was allowed to equilibrate with cells for 15–30 min. After the equilibration period, the media in the luminal chamber were replaced with warm PRF EBM containing 10 mg/ml FITC-Dx 70.

To determine the baseline flux of FITC-Dx 70, 20-μl samples were taken from the abluminal chamber at 0, 15, 30, 45, and 60 min. In some experiments, pharmacological inhibitors were added at the beginning of the baseline period. Flux was calculated as the slope of the best-fit line of accumulated FITC-Dx 70 versus time, using the least-squares method. After the 60-min baseline period, 1 nM VEGF, 100 μM SNAP, or the appropriate vehicle was added to the chamber, and 20-μl abluminal samples were taken at 65, 75, 90, 105, and 120 min to determine FITC-Dx 70 flux. In some experiments, the pharmacological inhibitor of interest was added after the 60-min baseline period, in place of VEGF, to determine any direct effect of the inhibitor. Samples (5 μl) from the luminal chamber were taken at 0, 55, and 120 min to determine the luminal concentration of FITC-Dx 70. The samples were diluted in 1 ml distilled water, and the amount of FITC-Dx 70 present was determined with a Perkin-Elmer Fluorescence Spectrophotometer (LS-3, Perkin-Elmer; Norwalk, CT). Permeability of the monolayer to FITC-Dx 70 was

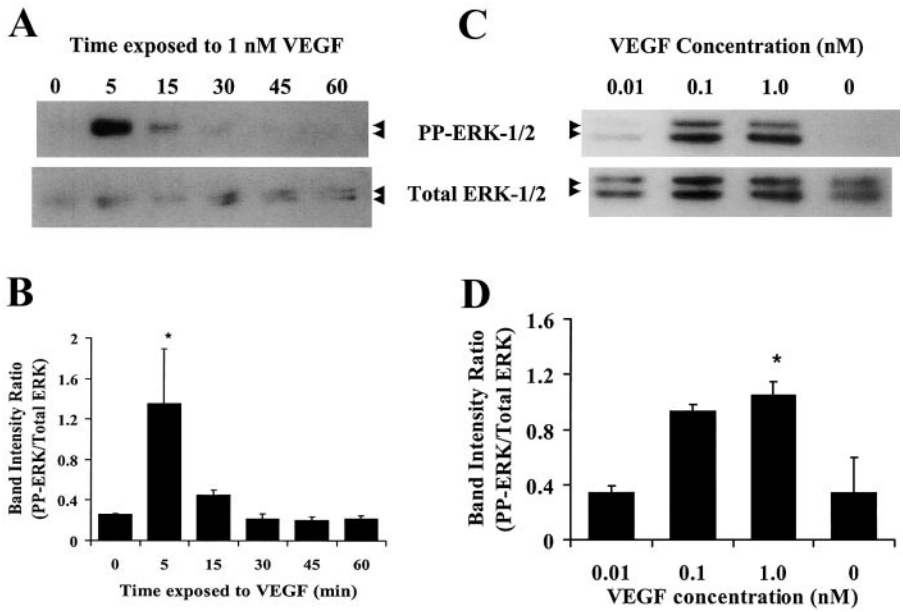

Fig. 1. Time course and concentration dependence of VEGF-induced ERK-1/2 activation. *A*: confluent human umbilical vein endothelial cell (HUVEC) monolayers were serum-starved for 16 h and then exposed to 1 nM VEGF for the indicated durations. The active form of ERK-1/2 was detected by immunoblotting with antibodies against the dually phoshorylated (PP) activation site of ERK-1/2 (phosphorylated Thr-183 and Tyr-185). Blots were reprobed with anti-ERK-1/2 to show total ERK protein. *B*: ratio of PP-ERK to total ERK was calculated for each time point. *C*: HUVEC were serum starved for 16 h and exposed to the indicated concentrations of VEGF for 5 min. PP-ERK-1/2 and total ERK-1/2 were detected as described above, and the ratio of PP-ERK-1/2 to total ERK-1/2 is shown in *D*. Results shown are representative of 3 experiments. $^*P < 0.05$ compared with control.

calculated from Fick's First Law of Diffusion [$P = J/A\Delta C$, where P is the permeability coefficient, J is solute flux (movement of FITC-Dx 70/time), A is the area of the endothelialized filter, and ΔC is the concentration difference across the monolayer and filter]. ΔC was approximated as the luminal concentration of FITC-Dx 70, because the amount of FITC-Dx 70 on the abluminal side is negligible compared with the luminal compartment.

Pharmacological inhibitors. PD-98059 and GW-5074 were used to block MEK and Raf-1, respectively. PD-98059 is a selective inhibitor of MEK and can effectively attenuate ERK-1/2 activation by growth factors at a range of 10–100 μM (2, 29). We used a concentration of 20 μM PD-98059, which has previously been demonstrated to inhibit VEGF-mediated permeability (21). GW-5074 is a novel inhibitor of Raf-1 that blocks ERK-1/2 activation at a concentration of 5 μM (24). We tested concentrations of 0.5, 1, and 5 μM GW-5074 in our ERK-1/2 phosphorylation experiments. To test the involvement of PKC pathways in ERK-1/2 phosphorylation, we used BIM I, a broad PKC inhibitor. BIM I effectively blocks PKC activity at a range of 5–20 μM without affecting other protein kinases (41). We used BIM I at a concentration of 10 μM because it blocks PMA- and VEGF-induced hyperpermeability in isolated coronary venules (20, 45). In addition, we utilized an inactive form, BIM V, as a negative control.

To block NO production, we used the arginine analog L-NAME. We and others have shown that 100 μM N^{ω}-monomethyl-L-arginine (L-NMMA) effectively blocks PKC-mediated microvascular hyperpermeability (20, 33) and platelet activating factor-mediated hyperpermeability (34). In addition, we have shown that 200 μM L-NMMA attenuates VEGF-mediated permeability in HUVEC monolayers (25). For the current study, we chose a concentration of 200 μM L-NAME to ensure blockade of NOS. To achieve a more complete assessment of the role of NO, we used SNAP as a donor, and PTIO as a NO scavenger. We used PTIO at concentrations ranging from 1 to 1,000 μM to test the role of NO in ERK-1/2 activation. PTIO effectively attenuates ACh-induced vasorelaxation over a concentration range of 100–300 μM (1).

Depletion of ERK-1/2 with antisense oligonucleotides. Phosphorothioate oligonucleotides were synthesized at the University of Medicine of New Jersey-New Jersey Medical School Molecular Resource Facility. HUVEC were grown to confluence in six-well plates or on polycarbonate membranes. The medium was replaced with serum-free OptiMEM containing 6 μl/ml TransIT-LT1 polyamine transfection reagent and 6 μg/ml of either ERK-1/2 antisense oligonucleotides (35) (5′-GCC GCC GCC GCC AT-3′), sense control oligonucleotides (5′-ATG GCG GCG GCG GCG-3′), or scrambled control oligonucleotides (5′-GCG GCG CTC GCG CAC CC-3′) for 3 h. The medium was then replaced with EGM containing 6 μg/ml of the appropriate oligonucleotide for an additional 16, 24, or 40 h, after which cells were either used for permeability experiments or harvested to measure the degree of ERK-1/2 depletion.

Immunoblot analysis. Protein was extracted on ice with a lysis buffer containing 1% Triton X-100, 50 mM Tris (pH 7.4), 150 mM NaCl, 0.1 mM EDTA, 0.1 mM EGTA, 1 mM PMSF, 10 μg/ml aprotinin, 10 μg/ml leupeptin, 1 mM Na_3VO_4, and 50 mM NaF in distilled water. After 15 min of incubation at 4°C, the lysate was centrifuged at 14,000 *g* for 15 min at 4°C, and the pellet was discarded. Protein concentrations of the supernatants were determined by the bicinchoninic acid protein assay. Supernatants were mixed 4:1 with 5× Laemmli sample buffer and boiled for 7 min. Equal amounts of protein for each sample were loaded into 10% polyacrylamide gels, separated by SDS-PAGE, and transferred to polyvinylidene difluoride (PVDF) membranes (Bio-Rad; Hercules, CA) by electrophoretic elution. Total ERK-1/2 or dually phosphorylated (Thr-183 and Tyr-185) ERK-1/2 was detected with the appropriate primary and secondary antibodies and visualized with the ECL system (Amersham). We performed this process by either reprobing the same PVDF membranes or using different membranes. Band intensities were determined using an IS-1,000 imaging system (Alpha Innotech; San Leandro, CA).

Statistical analysis. All data are presented as means ± SE. Permeability data are expressed as paired bars expressing mean permeability for the 1-h baseline period and the 1-h period after the addition of VEGF, SNAP, vehicle, etc. Immunoblot data are presented as a band intensity ratio of dually phosphorylated ERK-1/2 to total ERK-1/2. Groups

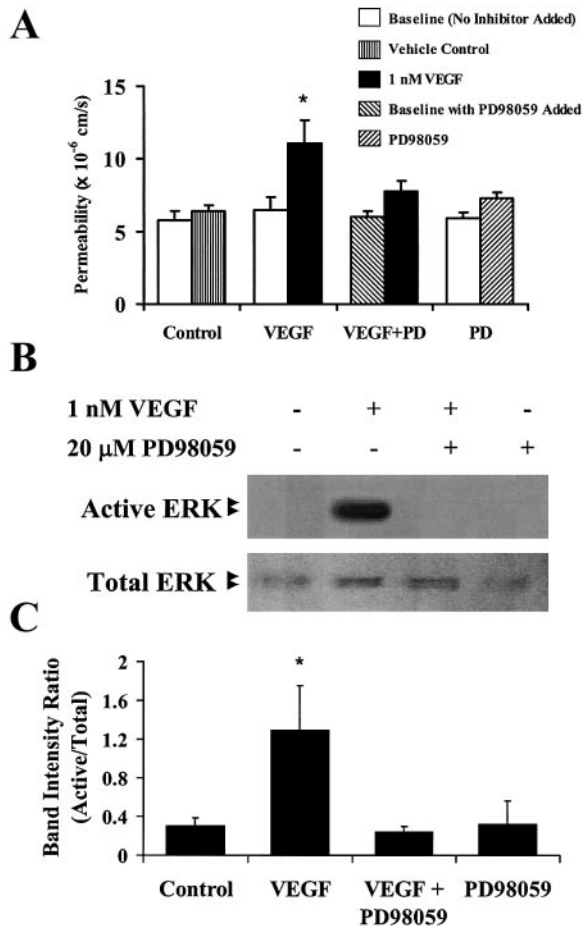

Fig. 2. MEK regulates VEGF-mediated hyperpermeability. *A*: HUVEC monolayers were pretreated with 20 μM PD-98059 for 1 h before the addition of 1 nM VEGF for an additional hour. The direct effect of PD-98059 was assessed by adding 20 μM PD-98059 after a 1-h baseline period. Data are expressed as the mean HUVEC permeability to FITC-Dextran 70 ± SE. For all groups, $n = 3$. *B*: confluent monolayers of HUVEC were serum starved for 16 h, pretreated with 20 μM PD-98059 for 1 h, and subsequently treated with 1 nM VEGF for 5 min. Activation of ERK-1/2 was determined by immunoblotting with anti-phospho-ERK-1/2 antibodies. The ratio of PP-ERK-1/2 to total ERK-1/2 (±SE) is shown in *C*. Results shown are representative of 3 experiments. $^*P < 0.05$ with respect to controls.

were analyzed for differences by one-way ANOVA, followed by Tukey's test. Significance was accepted at $P < 0.05$.

RESULTS

Time course of VEGF-induced phosphorylation of ERK-1/2. We first investigated the ability of VEGF to activate the ERK-1/2 signaling pathway by studying the time course of VEGF-induced phosphorylation of ERK-1/2 on Thr-183 and Tyr-185. VEGF caused a time-dependent increase in active ERK-1/2, as evidenced by immunoblotting with specific antibodies for the active, dually phosphorylated form of ERK-1/2 (Fig. 1). Maximal detection of phosphorylated ERK-1/2 was observed after a 5-min exposure to 1 nM VEGF, and a decline in ERK-1/2 activity was apparent by 15 min (Fig. 1, *A* and *B*). We have observed a similar time course of VEGF-mediated ERK-1/2 phosphorylation with adult human dermal microvascular endothelial cells (unpublished observations). VEGF-induced ERK-1/2 phosphorylation was concentration dependent over the range of 0.01–1.0 nM (Fig. 1, *C* and *D*). Because 1 nM VEGF produces a maximal response in our permeability model (25), we chose this concentration for further studies.

Signaling through ERK-1/2 in VEGF-induced hyperpermeability. VEGF at 1 nM increased the permeability of HUVEC monolayers to FITC-Dx 70. This increase was significantly attenuated by pretreatment with the selective MEK inhibitor PD-98059 (Fig. 2*A*). Pretreatment with 20 μM PD-98059 also effectively blocks VEGF-induced phosphorylation of ERK-1/2 at the activation site containing Thr-183 and Tyr-185 (Fig. 2, *B* and *C*). These data suggest a role for MEK in VEGF-induced hyperpermeability.

To further test whether ERK-1/2 signaling mediates VEGF-induced hyperpermeability, we depleted ERK-1/2 in HUVEC monolayers with antisense DNA oligonucleotides directed against ERK-1/2 and examined permeability changes in response to VEGF. Treatment of HUVEC with antisense oligonucleotides directed against ERK-1/2 for 16 or 24 h partially reduced ERK-1/2 protein, whereas treatment for 40 h depleted ERK-1/2 to an undetectable level (Fig. 3*A*). ERK-1/2 depletion was not observed on treatment with sense or scrambled control oligonucleotides for 40 h (Fig. 3*B*). Depletion of ERK-1/2 protein by 40 h of antisense oligonucleotide treatment also abolished VEGF-induced hyperpermeability, whereas sense and scrambled control oligonucleotides did not (Fig. 3*C*). These results indicate that VEGF-induced hyperpermeability is mediated by ERK-1/2.

Role of upstream mediators of ERK-1/2 in VEGF-induced hyperpermeability. We next investigated the roles of Raf-1 and PKC in VEGF-induced ERK-1/2 activation and hyperpermeability. To block Raf-1, a direct regulator of MEK, we used a novel, selective Raf-1 kinase inhibitor, GW-5074 (24). Pretreatment of HUVEC for 1 h with 0.5 or 1 μM GW-5074 attenuated VEGF-induced ERK-1/2 phosphorylation, whereas 5 μM GW-5074 abolished VEGF-induced ERK-1/2 phosphorylation (Fig. 4, *A* and *B*). GW-5074 also significantly attenuated VEGF-induced hyperpermeability (Fig. 4*C*).

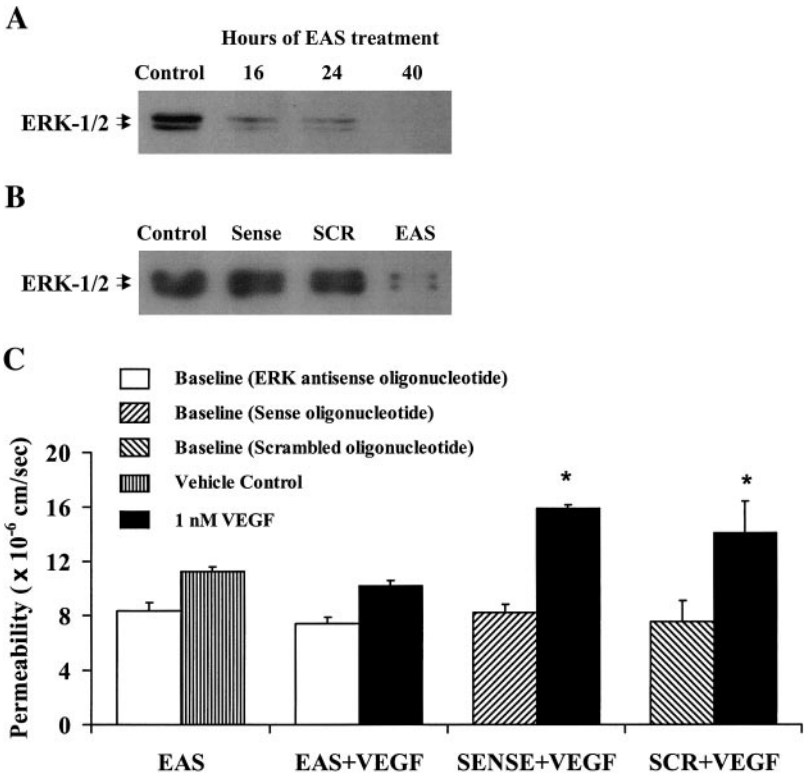

Fig. 3. Depletion of ERK-1/2 from HUVEC monolayers abolishes VEGF-induced hyperpermeability. *A*: time course of inhibition of ERK-1/2 expression by antisense treatment. After an initial incubation with ERK antisense oligonucleotides plus TransIT-LT1, cells were incubated with ERK antisense oligonucleotides (EAS) alone for the indicated times. Incubation with scrambled (SCR) or sense control oligonucleotides (sense) did not affect ERK-1/2 expression (*B*). Results shown are representative of 3 experiments. *C*: confluent HUVEC monolayers were treated with ERK antisense or control oligonucleotides for 40 h, and permeability was determined for a 60-min baseline period, followed by a 60-min period in the presence of 1 nM VEGF or vehicle. For all groups, $n = 3$. $^*P < 0.05$ with respect to paired baseline.

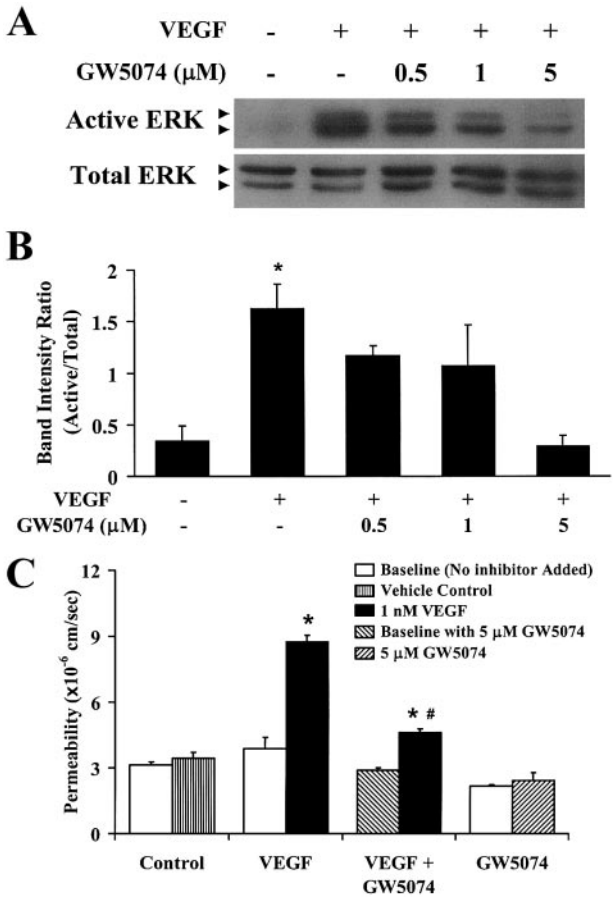

Fig. 4. Raf-1 mediates VEGF-induced ERK-1/2 activation and hyperpermeability. *A*: confluent HUVEC were pretreated for 1 h with 0.5, 1, or 5 μM GW-5074 and subsequently treated for 5 min with 1 nM VEGF. Activation of ERK-1/2 was assessed by immunoblotting for the diphosphorylated, active form of ERK-1/2. *B*: mean ratios of PP-ERK-1/2 to total ERK-1/2 (±SE) from 3 experiments are shown for each group. *C*: confluent HUVEC monolayers were pretreated for 1 h with 5 μM GW-5074 before the addition of 1 nM VEGF. The direct effect of GW-5074 was assessed by adding 5 μM GW-5074 after a 1-h baseline period. Data are expressed as means HUVEC permeability to FITC-Dextran 70 ± SE. For all groups, $n = 3$. *$P < 0.05$ with respect to controls; #$P < 0.05$ with respect to 1 nM VEGF without GW-5074.

PKC has been described as a direct upstream mediator of Raf-1 (9). We tested the role of PKC in VEGF-induced hyperpermeability and ERK-1/2 activation. The selective PKC inhibitor BIM I (10 μM) abolished VEGF-induced phosphorylation of ERK-1/2, whereas an inactive bisindolylmaleimide, BIM V, did not (Fig. 5, *A* and *B*). In addition, pretreatment of HUVEC with 10 μM BIM I also abolished VEGF-induced hyperpermeability (Fig. 5*C*), whereas BIM V had no effect.

NO and VEGF-induced ERK-1/2 activation. We have previously shown that inhibition of NOS abolishes PKC-mediated changes in permeability (33) and VEGF-induced hyperpermeability (25). We therefore tested whether VEGF-induced increases in ERK-1/2 phosphorylation are mediated by NOS. Pretreatment of HUVEC with 200 μM L-NAME for 1 h did not affect the increase in phosphorylation of ERK-1/2 caused by 1 nM VEGF (Fig. 6, *A* and *B*). However, L-NAME pretreatment did block VEGF-induced hyperpermeability (Fig. 6*C*), consistent with our previous data (25).

To further test the role of NO in VEGF-induced ERK-1/2 activation and hyperpermeability, we pretreated HUVEC with PTIO, a scavenger of NO. Treatment with PTIO did not significantly affect VEGF-induced ERK-1/2 activation (Fig. 7, *A* and *B*). In contrast, pretreatment of HUVEC with 100 μM PTIO blocked VEGF-induced hyperpermeability (Fig. 7*C*).

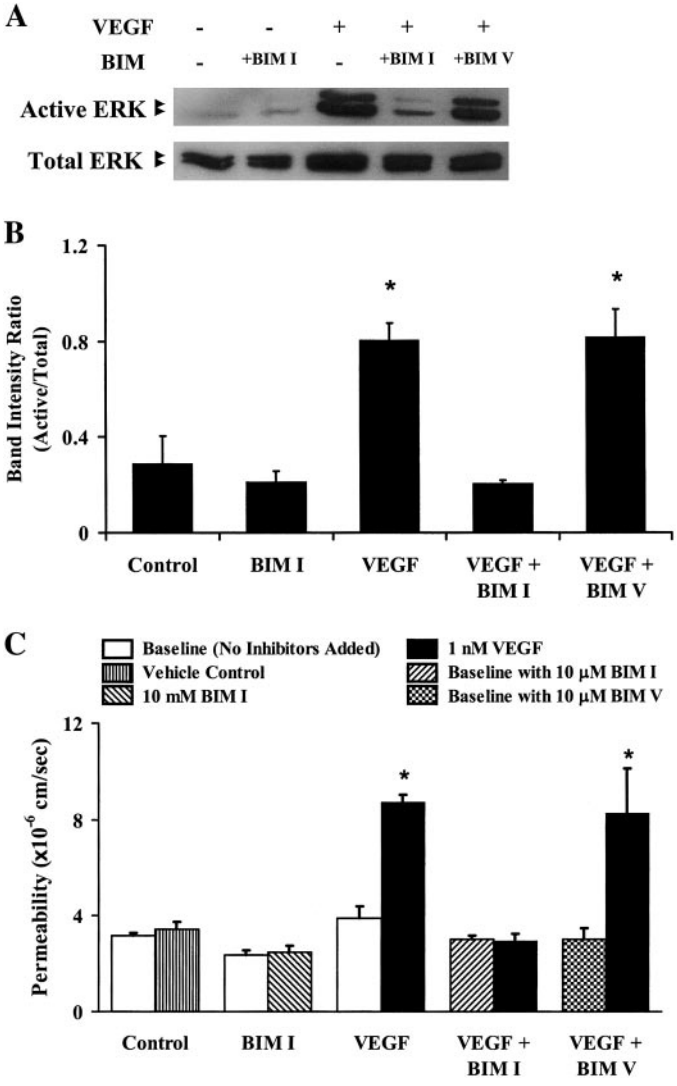

Fig. 5. Inhibition of PKC blocks VEGF-induced ERK-1/2 activation and hyperpermeability. *A*: confluent HUVEC were pretreated with 10 μM bisindolylmaleimide I (BIM I) or 10 μM BIM V for 1 h, followed by treatment with 1 nM VEGF for 5 min. PP-ERK-1/2 and total ERK-1/2 were detected by immunoblotting. *B*: mean ratio (±SE) of PP-ERK-1/2 to total ERK-1/2 was calculated for each group. *C*: confluent HUVEC monolayers were pretreated for 1 h with 10 μM BIM I before the addition of 1 nM VEGF. The direct effect of BIM I was assessed by adding 10 μM BIM I after a 1-h baseline period. Data are expressed as means HUVEC permeability to FITC-Dextran 70 ± SE. For all groups, $n = 3$. *$P < 0.05$ compared with all other groups.

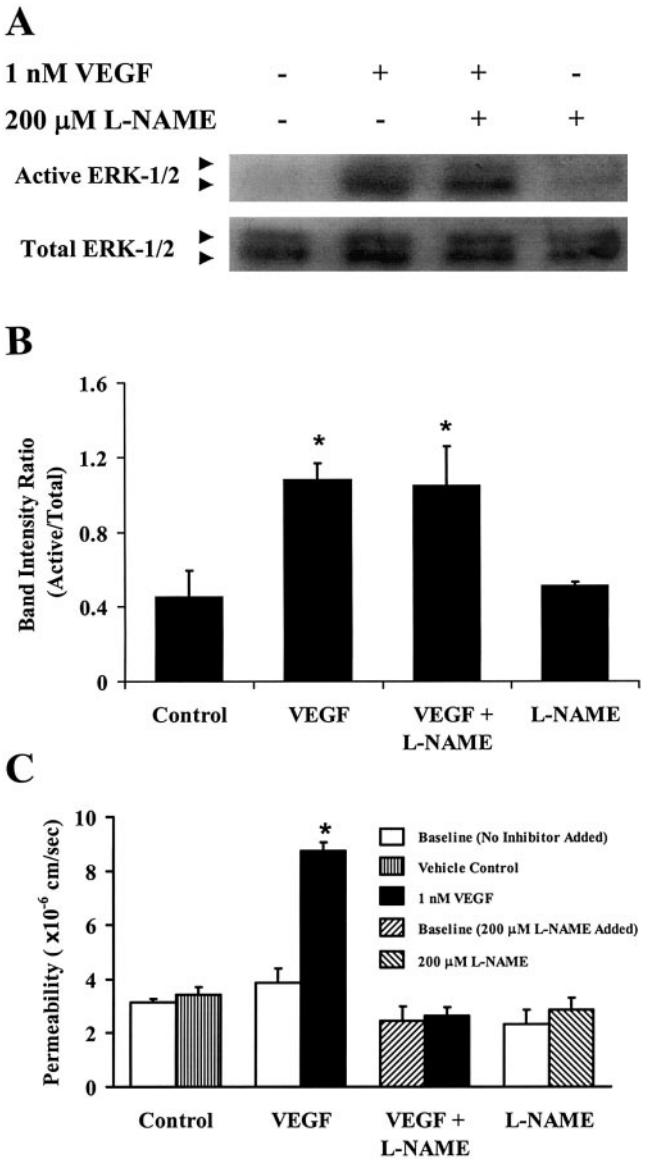

Fig. 6. Inhibition of nitric oxide (NO) synthase does not block VEGF-induced ERK-1/2 activation but abolishes VEGF-mediated hyperpermeability. *A*: confluent HUVEC were pretreated with 200 μM N^G-nitro-L-arginine methyl ester (L-NAME) for 1 h, followed by treatment with 1 nM VEGF for 5 min. PP-ERK-1/2 and total ERK-1/2 were detected by immunoblotting, and the mean (±SE) ratio of PP-ERK-1/2 to total ERK-1/2 for each group (*B*) was determined. *C*: confluent HUVEC monolayers were pretreated for 1 h with 200 μM L-NAME before the addition of 1 nM VEGF. The direct effect of L-NAME was assessed by adding 200 μM L-NAME after a 1-h baseline period. Data are expressed as means HUVEC permeability to FITC-Dextran 70 ± SE. For all groups, $n = 3$. *$P < 0.05$ compared with controls.

These observations suggest that NO production is not necessary for VEGF-induced ERK-1/2 activation, but NO does have an important role as a mediator of VEGF-induced increases in permeability.

Exogenous NO, ERK-1/2 activation, and permeability. Because other investigators have suggested that VEGF-induced ERK-1/2 activation may occur via the NOS-cGMP pathway (19, 30), we also tested the ability of exogenous NO to activate the ERK-1/2 pathway and to increase permeability in our model. When applied at 10 μM, the NO donor SNAP caused a slight increase in ERK-1/2 phosphorylation ($P = 0.09$ compared with controls), which peaked at 1–3 min and returned to baseline by 5 min (Fig. 8, *A* and *B*). This small increase in ERK-1/2 phosphorylation was markedly less than the degree of ERK-1/2 phosphorylation caused by 1 nM VEGF.

Application of 10 μM SNAP significantly increased HUVEC permeability, but VEGF did not affect permeability when applied at 2 μM (Fig. 8*C*). Interestingly, pretreatment of HUVEC monolayers for 1 h with 20 μM PD-98059 attenuated SNAP-mediated hyperper-

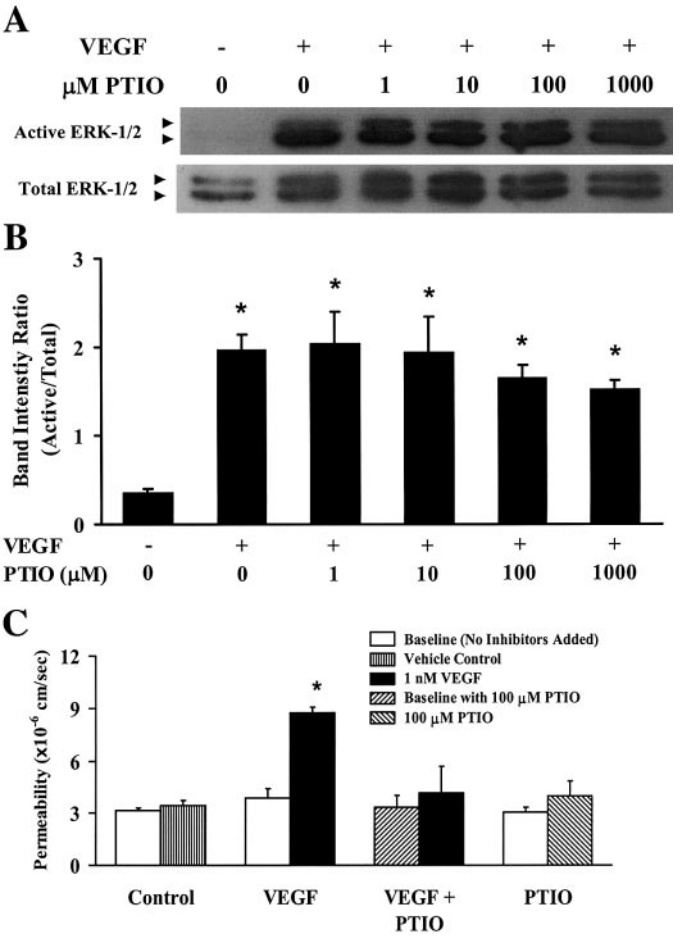

Fig. 7. Depletion of NO does not block VEGF-mediated ERK-1/2 activation but does attenuate VEGF-induced hyperpermeablity. *A*: confluent HUVEC were pretreated for 1 h with the indicated concentrations of 2-phenyl-4,4,5,5-tetramethylimidazoline-1-oxyl-3-oxide (PTIO; a NO scavenger) and subsequently treated for 5 min with 1 nM VEGF. Activation of ERK-1/2 was assessed by immunoblotting for the diphosphorylated, active form of ERK-1/2. *B*: mean ratios (±SE) of PP-ERK-1/2 to total ERK-1/2 from 3 experiments are shown for each group. *C*: HUVEC monolayers were pretreated with 100 μM PTIO for 1 h before the addition of 1 nM VEGF for an additional hour. The direct effect of PTIO was assessed by adding 100 μM PTIO after a 1-h baseline period. Data are expressed as means HUVEC permeability to FITC-Dextran 70 ± SE. For all groups, $n = 3$. *$P <$ 0.05 with respect to controls.

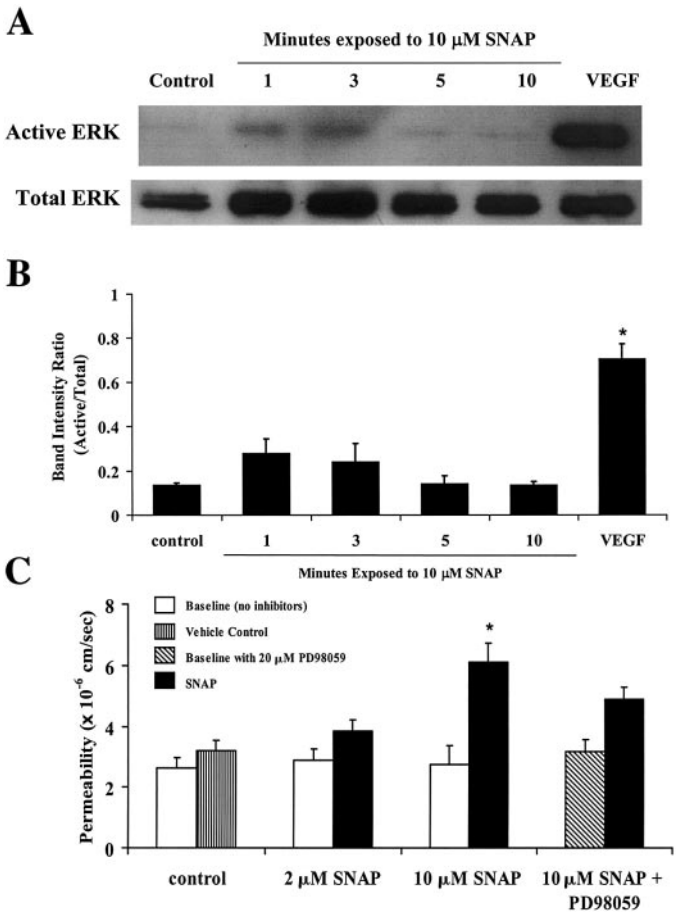

Fig. 8. Exogenous NO increases permeability and weakly activates ERK-1/2. *A*. HUVEC monolayers were treated for 1 h with 2 or 10 μM *S*-nitroso-*N*-acetyl penicillamine (SNAP) after a baseline period of 1 h. For one group, cells were pretreated for 1 h with 20 μM PD-98059 before the addition of 10 μM SNAP. Data are expressed as means HUVEC permeability to FITC-Dextran 70 ± SE. For the control and 10 μM SNAP groups, $n = 3$; for the 2 μM SNAP group, $n = 7$; and for the SNAP + PD-98059 group, $n = 4$. *B*: confluent HUVEC were serum starved for 16 h and then treated with 10 μM SNAP for the indicated times. HUVEC exposed to 1 nM VEGF for 5 min are also shown for comparison. Activation of ERK-1/2 was assessed by immunoblotting for the diphosphorylated, active form of ERK-1/2. Mean ratios of PP-ERK-1/2 to total ERK-1/2 were calculated for each group. For each group, $n = 4$. Data are expressed as means ± SE. $^*P < 0.05$ with respect to controls.

meability. These data suggest that exogenous NO increases permeability in part by activating MEK-dependent pathways, but also by other signaling targets that are independent of the MEK-dependent pathways.

DISCUSSION

We demonstrated here that ERK-1/2 mediates the VEGF signaling cascade leading to increased permeability in vitro. Our demonstration is based on the ability of both pharmacological blockade of ERK-1/2 activity and depletion of ERK-1/2 by antisense oligonucleotides to abolish VEGF-induced hyperpermeability. We also documented that Raf-1 and PKC, two recognized upstream mediators in the ERK-1/2 pathway, participate in both VEGF-induced ERK-1/2 activation and hyperpermeability. In addition, we have shown that NO, although an important mediator of VEGF-induced hyperpermeability, does not seem to have a significant role in VEGF-induced ERK-1/2 activation. Furthermore, we have demonstrated that SNAP-induced hyperpermeability can be attenuated by blockade of MEK. Our results support the hypothesis that VEGF causes increased permeability through at least two pathways: one including PKC, Raf-1, MEK, and ERK-1/2; and the other including PKC and NOS. Our data also support the hypothesis that areas of cross-talk exist between these two pathways.

Our studies of the time course for VEGF-induced activation of the ERK-1/2 pathway showed a time-dependent increase in the dually phosphorylated, active form of ERK-1/2. The amount of phosphorylated ERK-1/2 was maximal 5 min after administration of 1 nM VEGF and decreased back to control levels 30 min afterward. Other investigators have reported a similar time course of VEGF-induced ERK-1/2 activation, using two- to fourfold higher concentrations of VEGF (5, 18). We also demonstrated that VEGF-induced ERK-1/2 activation is concentration dependent. Although 0.01 nM VEGF produced little ERK-1/2 activation, concentrations of 0.1 and 1.0 nM VEGF reached a plateau at a significantly higher level of phosphorylation.

Our study is the first to demonstrate that depletion of ERK-1/2 with antisense oligonucleotides can inhibit VEGF-induced hyperpermeability. These data are consistent with our demonstration that pharmacological inhibitors of MEK and Raf-1, two well-described upstream mediators of ERK-1/2, block VEGF-induced hyperpermeability. Our results are concordant with the results of other studies using endothelial cell monolayer models (5, 21, 25, 42, 43). However, in studies using frog microvessels, ERK-1/2 inhibition failed to block a VEGF-induced increase in hydraulic conductivity coefficient (3, 31). This discrepancy may be due to differences in experimental models and species.

We also showed that inhibition of PKC blocks VEGF-induced hyperpermeability. These data are in agreement with studies documenting PKC as a mediator of microvascular permeability (10, 22, 33, 40, 43, 45, 47). One recent study (37) has suggested that PKC blockade enhances VEGF-induced hyperpermeability. However, this observation relies on protein extravasation data from the Miles assay, which lacks the necessary controls over blood flow to make accurate conclusions about microvascular permeability.

The eNOS-cGMP pathway for regulation of endothelial permeability is well established (20, 25, 33, 34, 42, 44). In porcine coronary venular endothelial cells, inhibition of NOS blocks activation of ERK-1/2 by VEGF (30). There is also evidence that the NO-cGMP-PKG pathway activates Raf-1 (19). We and others have demonstrated that inhibition of NOS blocks VEGF-induced hyperpermeability (25, 44). In the present study, inhibition of NOS with L-NAME blocked VEGF-

induced hyperpermeability but failed to block VEGF-induced ERK-1/2 phosphorylation in HUVEC. Although this observation is in contrast to previous findings using porcine coronary venular endothelial cells (30), it is concordant with studies in HUVEC (16). Our results suggest that NO does not modulate VEGF-induced ERK-1/2 phosphorylation. This finding, however, may not be true for all endothelial cell types.

It is also worth noting that the role of NO in ERK-1/2 activation may vary for different agonists. Activation of the NO-cGMP pathway with cGMP analogs promotes increased permeability across HUVEC monolayers by a mechanism involving ERK-1/2 (42). In the present study, exogenous NO caused increased permeability and a weak phosphorylation of ERK-1/2. Also, blockade of the ERK-1/2 pathway attenuated SNAP-induced hyperpermeability.

The precise sequence of events in the regulation of endothelial permeability remains unclear. A recent biochemical study (6) shows that dissociation of the ERK-1/2-eNOS complex on stimulation with bradykinin leads to eNOS activation. Therefore, it is possible that ERK-1/2 may regulate permeability by influencing eNOS activity. Another likely possibility is that the NO pathway acts in parallel to the ERK-1/2 pathway in VEGF-induced hyperpermeability, with areas of cross-talk. These pathways may in turn influence the different biochemical components of endothelial cells that work concomitantly in the regulation of permeability, namely, junctional proteins, the cytoskeleton, and focal adhesion proteins (46).

In summary, we demonstrated, by depletion of ERK-1/2 protein with an antisense strategy, that the ERK-1/2 pathway mediates VEGF-induced endothelial hyperpermeability. We propose that VEGF-induced, NO-mediated enhancement of permeability is associated with a separate signaling pathway largely independent of ERK-1/2 phosphorylation. Our data support the existence of areas of cross-talk between these two pathways.

This work was supported by National Heart, Lung, and Blood Institute Grants 1RO1-HL-70634, KO8-HL-03354, and KO7-HL-03437 and by a Faculty Development Grant from the Department of Surgery at the New Jersey Medical School.

REFERENCES

1. **Akaike T, Yoshida M, Miyamoto Y, Sato K, Kohno M, Sasamoto K, Miyazaki K, Ueda S, and Maeda H.** Antagonistic action of imidazolineoxyl *N*-oxides against endothelium-derived relaxing factor. NO through a radical reaction. *Biochemistry* 32: 827–832, 1993.
2. **Alessi DR, Cuenda A, Cohen P, Dudley DT, and Saltiel AR.** PD 098059 is a specific inhibitor of the activation of mitogen-activated protein kinase kinase in vitro and in vivo. *J Biol Chem* 270: 27489–27494, 1995.
3. **Bates DO, Heald RI, Curry FE, and Williams B.** Vascular endothelial growth factor increases Rana vascular permeability and compliance by different signalling pathways. *J Physiol* 533: 263–272, 2001.
4. **Bates DO, Lodwick D, and Williams B.** Vascular endothelial growth factor and microvascular permeability. *Microcirculation* 6: 83–96, 1999.
5. **Becker PM, Verin AD, Booth MA, Liu F, Birukova A, and Garcia JG.** Differential regulation of diverse physiological responses to VEGF in pulmonary endothelial cells. *Am J Physiol Lung Cell Mol Physiol* 281: L1500–L1511, 2001.
6. **Bernier SG, Haldar S, and Michel T.** Bradykinin-regulated interactions of the mitogen-activated protein kinase pathway with the endothelial nitric-oxide synthase. *J Biol Chem* 275: 30707–30715, 2000.
7. **Berridge MJ.** Inositol trisphosphate and calcium signalling. *Nature* 361: 315–325, 1993.
8. **Brock TA, Dvorak HF, and Senger DR.** Tumor-secreted vascular permeability factor increases cytosolic Ca^{2+} and von Willebrand factor release in human endothelial cells. *Am J Pathol* 138: 213–221, 1991.
9. **Cobb MH.** MAP kinase pathways. *Prog Biophys Mol Biol* 71: 479–500, 1999.
10. **Cohen AW, Carbajal JM, and Schaeffer RC Jr.** VEGF stimulates tyrosine phosphorylation of β-catenin and small-pore endothelial barrier dysfunction. *Am J Physiol Heart Circ Physiol* 277: H2038–H2049, 1999.
11. **Dimmeler S, Fleming I, Fisslthaler B, Hermann C, Busse R, and Zeiher AM.** Activation of nitric oxide synthase in endothelial cells by Akt-dependent phosphorylation. *Nature* 399: 601–605, 1999.
12. **Doanes AM, Hegland DD, Sethi R, Kovesdi I, Bruder JT, and Finkel T.** VEGF stimulates MAPK through a pathway that is unique for receptor tyrosine kinases. *Biochem Biophys Res Commun* 255: 545–548, 1999.
13. **Dvorak HF, Nagy JA, Berse B, Brown LF, Yeo KT, Yeo TK, Dvorak AM, Van De Water L, Sioussat TM, and Senger DR.** Vascular permeability factor, fibrin, and the pathogenesis of tumor stroma formation. *Ann NY Acad Sci* 667: 101–111, 1992.
14. **Franke TF, Kaplan DR, Cantley LC, and Toker A.** Direct regulation of the Akt proto-oncogene product by phosphatidylinositol-3,4-bisphosphate. *Science* 275: 665–668, 1997.
15. **Fulton D, Gratton JP, McCabe TJ, Fontana J, Fujio Y, Walsh K, Franke TF, Papapetropoulos A, and Sessa WC.** Regulation of endothelium-derived nitric oxide production by the protein kinase Akt. *Nature* 399: 597–601, 1999.
16. **Gliki G, Abu-Ghazaleh R, Jezequel S, Wheeler-Jones C, and Zachary I.** Vascular endothelial growth factor-induced prostacyclin production is mediated by a protein kinase C (PKC)-dependent activation of extracellular signal-regulated protein kinases 1 and 2 involving PKC-delta and by mobilization of intracellular Ca^{2+}. *Biochem J* 353: 503–512, 2001.
17. **Guo D, Jia Q, Song HY, Warren RS, and Donner DB.** Vascular endothelial cell growth factor promotes tyrosine phosphorylation of mediators of signal transduction that contain SH2 domains. Association with endothelial cell proliferation. *J Biol Chem* 270: 6729–6733, 1995.
18. **Gupta K, Kshirsagar S, Li W, Gui L, Ramakrishnan S, Gupta P, Law PY, and Hebbel RP.** VEGF prevents apoptosis of human microvascular endothelial cells via opposing effects on MAPK/ERK and SAPK/JNK signaling. *Exp Cell Res* 247: 495–504, 1999.
19. **Hood J and Granger HJ.** Protein kinase G mediates vascular endothelial growth factor-induced Raf-1 activation and proliferation in human endothelial cells. *J Biol Chem* 273: 23504–23508, 1998.
20. **Huang Q and Yuan Y.** Interaction of PKC and NOS in signal transduction of microvascular hyperpermeability. *Am J Physiol Heart Circ Physiol* 273: H2442–H2451, 1997.
21. **Kevil CG, Payne DK, Mire E, and Alexander JS.** Vascular permeability factor/vascular endothelial cell growth factor-mediated permeability occurs through disorganization of endothelial junctional proteins. *J Biol Chem* 273: 15099–15103, 1998.
22. **Kobayashi I, Kim D, Hobson RW, and Durán WN.** Platelet-activating factor modulates microvascular transport by stimulation of protein kinase C. *Am J Physiol Heart Circ Physiol* 266: H1214–H1220, 1994.
23. **Kroll J and Waltenberger J.** The vascular endothelial growth factor receptor KDR activates multiple signal transduction path-

ways in porcine aortic endothelial cells. *J Biol Chem* 272: 32521–32527, 1997.
24. **Lackey K, Cory M, Davis R, Frye SV, Harris PA, Hunter RN, Jung DK, McDonald OB, McNutt RW, Peel MR, Rutkowske RD, Veal JM, and Wood ER.** The discovery of potent cRaf1 kinase inhibitors. *Bioorg Med Chem* 10: 223–226, 2000.
25. **Lal BK, Varma S, Pappas PJ, Hobson RW, and Durán WN.** VEGF increases permeability of the endothelial cell monolayer by activation of PKB/akt, endothelial nitric-oxide synthase, and MAP kinase pathways. *Microvasc Res* 62: 252–262, 2001.
26. **Mayhan WG.** VEGF increases permeability of the blood-brain barrier via a nitric oxide synthase/cGMP-dependent pathway. *Am J Physiol Cell Physiol* 276: C1148–C1153, 1999.
27. **Millauer B, Wizigmann-Voos S, Schnurch H, Martinez R, Moller NP, Risau W, and Ullrich A.** High affinity VEGF binding and developmental expression suggest Flk-1 as a major regulator of vasculogenesis and angiogenesis. *Cell* 72: 835–846, 1993.
28. **Mukhopadhyay D, Nagy JA, Manseau EJ, and Dvorak HF.** Vascular permeability factor/vascular endothelial growth factor-mediated signaling in mouse mesentery vascular endothelium. *Cancer Res* 58: 1278–1284, 1998.
29. **Pang L, Sawada T, Decker SJ, and Saltiel AR.** Inhibition of MAP kinase kinase blocks the differentiation of PC-12 cells induced by nerve growth factor. *J Biol Chem* 270: 13585–13588, 1995.
30. **Parenti A, Morbidelli L, Cui XL, Douglas JG, Hood JD, Granger HJ, Ledda F, and Ziche M.** Nitric oxide is an upstream signal of vascular endothelial growth factor-induced extracellular signal-regulated kinase1/2 activation in postcapillary endothelium. *J Biol Chem* 273: 4220–4226, 1998.
31. **Pocock TM and Bates DO.** In vivo mechanisms of vascular endothelial growth factor-mediated increased hydraulic conductivity of Rana capillaries. *J Physiol* 534: 479–488, 2001.
32. **Quinn TP, Peters KG, De Vries C, Ferrara N, and Williams LT.** Fetal liver kinase 1 is a receptor for vascular endothelial growth factor and is selectively expressed in vascular endothelium. *Proc Natl Acad Sci USA* 90: 7533–7537, 1993.
33. **Ramírez MM, Kim DD, and Durán WN.** Protein kinase C modulates microvascular permeability through nitric oxide synthase. *Am J Physiol Heart Circ Physiol* 271: H1702–H1705, 1996.
34. **Ramírez MM, Quardt SM, Kim D, Oshiro H, Minnicozzi M, and Durán WN.** Platelet activating factor modulates microvascular permeability through nitric oxide synthesis. *Microvasc Res* 50: 223–234, 1995.
35. **Sale EM, Atkinson PG, and Sale GJ.** Requirement of MAP kinase for differentiation of fibroblasts to adipocytes, for insulin activation of p90 S6 kinase and for insulin or serum stimulation of DNA synthesis. *EMBO J* 14: 674–684, 1995.
36. **Senger DR, Van De Water L, Brown LF, Nagy JA, Yeo KT, Yeo TK, Berse B, Jackman RW, Dvorak AM, and Dvorak HF.** Vascular permeability factor (VPF, VEGF) in tumor biology. *Cancer Metastasis Rev* 12: 303–324, 1993.
37. **Spyridopoulos I, Luedemann C, Chen D, Kearney M, Chen D, Murohara T, Principe N, Isner JM, and Losordo DW.** Divergence of angiogenic and vascular permeability signaling by VEGF: inhibition of protein kinase C suppresses VEGF-induced angiogenesis, but promotes VEGF-induced, NO-dependent vascular permeability. *Arterioscler Thromb Vasc Biol* 22: 901–906, 2002.
38. **Stephan CC and Brock TA.** Vascular endothelial growth factor, a multifunctional polypeptide. *P R Health Sci J* 15: 169–178, 1996.
39. **Takahashi T, Ueno H, and Shibuya M.** VEGF activates protein kinase C-dependent, but Ras-independent Raf-MEK-MAP kinase pathway for DNA synthesis in primary endothelial cells. *Oncogene* 18: 2221–2230, 1999.
40. **Tinsley JH, Zawieja DC, Wu MH, Ustinova EE, Xu W, and Yuan SY.** Protein transfection of intact microvessels specifically modulates vasoreactivity and permeability. *J Vasc Res* 38: 444–452, 2001.
41. **Toullec D, Pianetti P, Coste H, Bellevergue P, Grand-Perret T, Ajakane M, Baudet V, Boissin P, Boursier E, and Loriolle F.** The bisindolylmaleimide GF 109203X is a potent and selective inhibitor of protein kinase C. *J Biol Chem* 266: 15771–15781, 1991.
42. **Varma S, Breslin JW, Lal BK, Pappas PJ, Hobson RW, and Durán WN.** p42/44(MAPK) regulates baseline permeability and cGMP-induced hyperpermeability in endothelial cells. *Microvasc Res* 63: 172–178, 2002.
43. **Verin AD, Liu F, Bogatcheva N, Borbiev T, Hershenson MB, Wang P, and Garcia JG.** Role of ras-dependent ERK activation in phorbol ester-induced endothelial cell barrier dysfunction. *Am J Physiol Lung Cell Mol Physiol* 279: L360–L370, 2000.
44. **Wu HM, Huang Q, Yuan Y, and Granger HJ.** VEGF induces NO-dependent hyperpermeability in coronary venules. *Am J Physiol Heart Circ Physiol* 271: H2735–H2739, 1996.
45. **Wu HM, Yuan Y, Zawieja DC, Tinsley J, and Granger HJ.** Role of phospholipase C, protein kinase C, and calcium in VEGF-induced venular hyperpermeability. *Am J Physiol Heart Circ Physiol* 276: H535–H542, 1999.
46. **Yuan SY.** Signal transduction pathways in enhanced microvascular permeability. *Microcirculation* 7: 395–403, 2000.
47. **Yuan SY, Ustinova EE, Wu MH, Tinsley JH, Xu W, Korompai FL, and Taulman AC.** Protein kinase C activation contributes to microvascular barrier dysfunction in the heart at early stages of diabetes. *Circ Res* 87: 412–417, 2000.